^{64}Cu-DOTATATE for Noninvasive Assessment of Atherosclerosis in Large Arteries and Its Correlation with Risk Factors: Head-to-Head Comparison with ^{68}Ga-DOTATOC in 60 Patients

Catarina Malmberg*[1], Rasmus S. Ripa*[1], Camilla B. Johnbeck[1], Ulrich Knigge[2], Seppo W. Langer[3], Jann Mortensen[1], Peter Oturai[1], Annika Loft[1], Anne Mette Hag[1], and Andreas Kjær[1]

[1]*Department of Clinical Physiology, Nuclear Medicine & PET, Rigshospitalet & Cluster for Molecular Imaging, University of Copenhagen, Copenhagen, Denmark;* [2]*Department of Surgical Gastroenterology C & Department of Endocrinology, Rigshospitalet, Copenhagen, Denmark; and* [3]*Department of Oncology, Rigshospitalet, Copenhagen, Denmark*

The somatostatin receptor subtype 2 is expressed on macrophages, an abundant cell type in the atherosclerotic plaque. Visualization of somatostatin receptor subtype 2, for oncologic purposes, is frequently made using the DOTA-derived somatostatin analogs DOTATOC or DOTATATE for PET. We aimed to compare the uptake of the PET tracers ^{68}Ga-DOTATOC and ^{64}Cu-DOTATATE in large arteries, in the assessment of atherosclerosis by noninvasive imaging technique, combining PET and CT. Further, the correlation of uptake and cardiovascular risk factors was investigated. **Methods:** Sixty consecutive patients with neuroendocrine tumors underwent both ^{68}Ga-DOTATOC and ^{64}Cu-DOTATATE PET/CT scans, in random order. For each scan, the maximum and mean standardized uptake values (SUVs) were calculated in 5 arterial segments. In addition, the blood-pool–corrected target-to-background ratio was calculated. Uptake of the tracers was correlated with cardiovascular risk factors collected from medical records. **Results:** We found detectable uptake of both tracers in all arterial segments studied. Uptake of ^{64}Cu-DOTATATE was significantly higher than ^{68}Ga-DOTATOC in the vascular regions both when calculated as maximum and mean uptake. There was a significant association between Framingham risk score and the overall maximum uptake of ^{64}Cu-DOTATATE using SUV ($r = 0.4$; $P = 0.004$) as well as target-to-background ratio ($r = 0.3$; $P = 0.04$), whereas no association was found with ^{68}Ga-DOTATOC. The association of risk factors and maximum SUV of ^{64}Cu-DOTATATE was found driven by body mass index, smoking, diabetes, and coronary calcium score ($P < 0.001$, $P = 0.01$, $P = 0.005$, and $P = 0.03$, respectively). **Conclusion:** In a series of oncologic patients, vascular uptake of ^{68}Ga-DOTATOC and ^{64}Cu-DOTATATE was found, with highest uptake of the latter. Uptake of ^{64}Cu-DOTATATE, but not of ^{68}Ga-DOTATOC, was correlated with cardiovascular risk factors, suggesting a potential role for ^{64}Cu-DOTATATE in the assessment of atherosclerosis.

Key Words: PET/CT; atherosclerosis; molecular imaging; somatostatin receptor; macrophages

J Nucl Med 2015; 56:1895–1900
DOI: 10.2967/jnumed.115.161216

Atherosclerosis is a systemic condition that can evolve to manifest cardiovascular disease, with potential fatal stroke or myocardial infarction as a result. Even though atherosclerosis is defined as a systemic condition, it consists of localized progressive plaques that can give rise to symptoms or proceed in a silent asymptomatic stage (*1*). The standard diagnosis of atherosclerosis includes physical examination; diagnostic tests such as blood tests, electrocardiogram, ankle/brachial index, and ultrasound; and invasive tests such as angiography, intravascular coronary ultrasound, and angioscopy (*2,3*). The examinations all vary in sensitivity, specificity, reproducibility, and availability. With emerging research identifying and unraveling cellular and molecular mechanisms of the changes in the progressive atherosclerotic plaque, new doors in diagnosing both clinical and subclinical stages of the disease have opened. Further, findings of molecular targets and cellular markers that are involved in the disease have led to development of new and noninvasive diagnostic techniques.

One particular target is the macrophage, which is an abundant cell type in the plaque and highly active in inflammation, a key process in progressive atherosclerosis. The macrophage migrates into the arterial intima as a monocyte where it matures to become a phagocytic macrophage. Various processes and cellular targets involved with the presence of this cell type have been investigated and identified as targets for PET, with expression of the somatostatin receptor, a G-protein–coupled 7-transmembrane protein, being one of them. Five human somatostatin receptors have been identified, and in atherosclerotic plaques the somatostatin receptor 2 is the most frequent (*4–6*). The somatostatin analogs DOTATOC and DOTATATE bind to somatostatin receptors, with highest affinity for the somatostatin receptor 2. Hence, they might be potential tracers for molecular imaging of atherosclerosis (*7,8*). A recent prospective study in patients with symptomatic carotid stenosis has indicated that uptake of ^{64}Cu-DOTATATE is a marker of activated macrophages within the plaque (*9*).

Received May 20, 2015; revision accepted Sep. 22, 2015.
For correspondence or reprints contact: Rasmus S. Ripa, Department of Clinical Physiology, Nuclear Medicine & PET, KF-4012 Rigshospitalet, Blegdamsvej 9, DK-2100 Copenhagen, Denmark.
E-mail: ripa@sund.ku.dk
*Contributed equally to this work.
Published online Oct. 1, 2015.

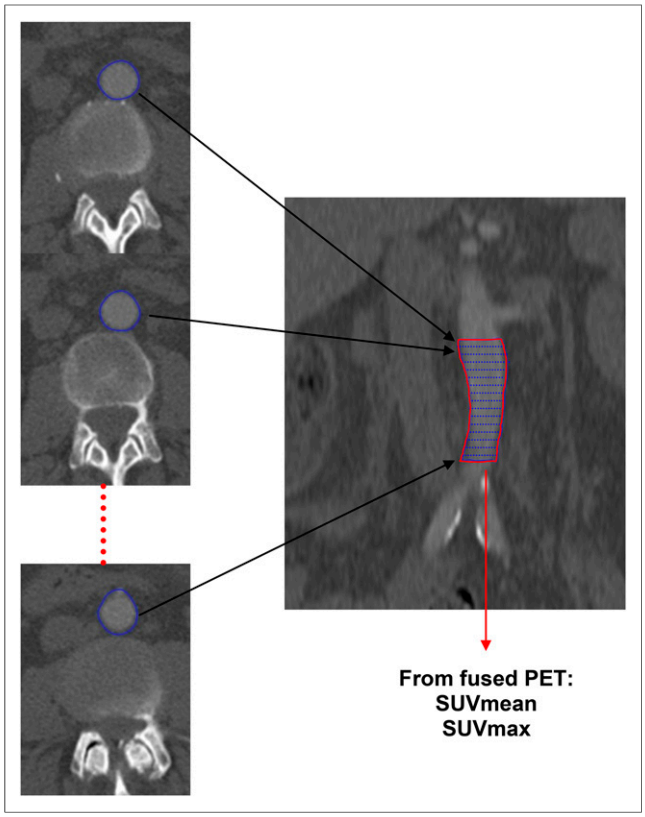

FIGURE 1. Method for vascular tracer uptake quantification. Example from distal abdominal aorta: 1. outer vessel wall is manually delineated on all consecutive axial slices; 2. imaging software fuses these consecutive ROIs into single 3D volume of interest covering distal abdominal aorta; 3. single SUV_{mean} and SUV_{max} are recorded for each volume of interest.

In our study, DOTATOC was labeled with the radionuclide ^{68}Ga and DOTATATE with ^{64}Cu. ^{68}Ga is produced by a ^{68}Ge/^{68}Ga generator that can last up to 9–12 mo because of the ^{68}Ge half-life of approximately 270 d. ^{68}Ga has a physical half-life of 68 min, which is compatible with the kinetics of most peptides. This makes ^{68}Ga a favorable positron emitter, independent of an on-site cyclotron and with fast target localization and blood clearance, with mainly excretion through the kidneys. ^{64}Cu, on the other hand, is generated on a cyclotron and has a half-life of 12.7 h. The long half-life of ^{64}Cu allows for early as well as late PET scanning, even the day after injection. ^{64}Cu has a substantially shorter positron range than ^{68}Ga, 1 versus 4 mm, rendering it a much better spatial resolution, but a lower positron abundance (*10–14*).

The objective of this study was to evaluate the use of 2 somatostatin receptor–binding PET tracers in the assessment of the large arteries. The uptake of the tracers was compared in various vascular regions and the correlation with known cardiovascular risk factors was investigated, to support the hypothesis that vascular lesions containing macrophages are present in individuals with a recognized risk for atherosclerosis.

MATERIALS AND METHODS

Study Design and Patient Selection

We performed the analysis on scans from an ongoing clinical trial comparing ^{68}Ga-DOTATOC and ^{64}Cu-DOTATATE PET/CT in patients with neuroendocrine tumors. All patients (n = 60) included in the original trial were included in the present substudy. The original inclusion criterion was verified neuroendocrine tumor with clinical indication for ^{111}In-octreotide SPECT/CT. Exclusion criteria were age below 18 y, pregnancy/lactation, performance status 0–2, and chemotherapy or radiation therapy in the previous 5 wk.

The study protocol complied with the Declaration of Helsinki (version 2013) and was approved by the Regional Scientific Ethical Committee. Written informed consent was obtained from all participants (protocol number H-D-2008-045).

For this substudy, the patients were reviewed regarding the 2 PET/CT scans, and known cardiovascular risk factors were collected retrospectively from their medical records. The investigated cardiovascular risk factors included age, sex, body mass index (BMI), smoking habits, diabetes, arterial hypertension defined by ongoing treatment, and hypercholesterolemia defined as ongoing treatment hereof. Because of few available cholesterol levels, the Framingham risk score was calculated by use of BMI, according to the Framingham Heart Study (*15*).

Imaging Procedures and Analysis

All patients underwent hybrid PET/CT scanning with ^{68}Ga-DOTATOC and ^{64}Cu-DOTATATE, in random order as soon as possible but with a maximum of 60 d in between. Each patient underwent the 2 examinations on the same hybrid PET/CT scanner (Biograph mCT64; Siemens). For the ^{68}Ga-DOTATOC scan, 150 MBq were injected intravenously and, after 45 min, whole-body PET was performed in direct connection with a whole-body CT scan (120 kV; effective mAs, 40)

TABLE 1
Baseline Characteristics

Characteristic	*n*
No. of patients	60
Age (y)	
Mean	61
Range	31–81
Sex	
M	36
F	24
History of CAD (%)	4 (7%)
Diabetes mellitus (%)	10 (17%)
Hyperlipidemia (%)	8 (13%)
Hypertension* (%)	29 (48%)
Smokers (%)	
Current	17 (28%)
Ex	13 (22%)
Acetylsalicylic acid treatment (%)	17 (10/60)
BMI	
Mean	25.7
Range	17–38
Coronary calcium score	
Mean	227
Range	0–3,356

*Defined as ongoing treatment for hypertension.
CAD = coronary artery disease.

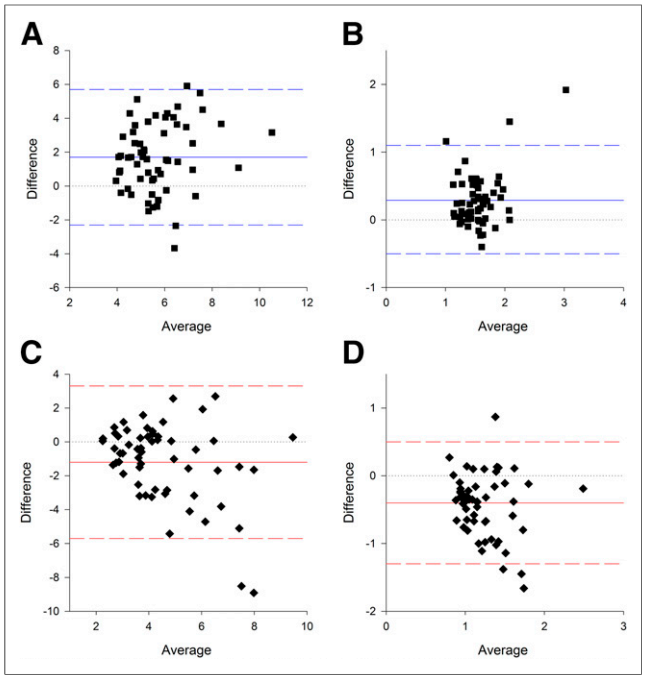

FIGURE 2. Comparison of ^{68}Ga-DOTATOC and ^{64}Cu-DOTATATE uptake in large arteries. Bland–Altman plots of difference, with dashed lines indicating identity line and horizontal colored lines indicating mean difference with 95% limits of agreement, are shown. Top line shows comparison of SUV_{max} (A) and SUV_{mean} (B). Likewise, bottom line shows comparison of maximum TBR (C) and mean TBR (D).

for attenuation correction of the PET and anatomic localization of the vessels. Likewise, the PET/CT scan after intravenous injection of 200 MBq of ^{64}Cu-DOTATATE was obtained 60 min after the injection. The PET scans were acquired in 3-dimensional (3D) list-mode for 3 min per bed position. The PET reconstruction settings were CT-based attenuation correction, resolution recovery (point-spread function, TrueX [Siemens]), and time of flight (3 iterations, 21 subsets; zoom, 1.0). A gaussian filter of 2 mm in full width at half maximum was then applied to all images after reconstruction.

Anatomic coregistration of CT and PET was carefully checked before the assessment of vascular tracer uptake. Uptake was determined in 5 distinct vascular segments (the aortic arch, the descending thoracic aorta, the proximal and distal abdominal aorta, and the common iliac arteries). For analysis, 3D regions of interest (ROIs) were drawn manually slice by slice on both scans in these particular regions using Inveon Research Workplace (version 4.1; Siemens), avoiding adjacent hot spots arisen from, for example, lymph nodal metastases. The mean and maximal standardized uptake value (SUV_{mean} and SUV_{max}, respectively) that correct for injected dose, patient weight, and time to acquisition were calculated for each 3D ROI (Fig. 1). In addition, each patient had whole-artery SUV_{mean} and whole-artery SUV_{max} calculated as the average of the 5 SUVs in each patient. The target-to-background ratio (TBR) was determined by dividing SUV of the vascular segment with SUV_{mean} from at least four 3D ROIs placed in the superior vena cava (representing the mean blood uptake).

The coronary artery calcium score was assessed using Syngo.via version VB 10A (Siemens Healthcare) and the Agatston equivalent method with an attenuation threshold of 130 Hounsfield units.

Statistical Analysis

Statistical analyses were made using SPSS statistics (version 22; IBM). The analysis and comparison of the uptake of the 2 tracers were made using the Bland–Altman method. According to this method, the mean difference between measurements is defined as bias and represents the systemic error in measurements. The statistical significance of the bias was assessed using the *t* test. The 95% limits of agreement were defined as mean difference ± 1.96 times the SD. All limits of agreement were calculated assuming normal distribution of the differences. The associations between tracer uptake and cardiovascular risk factors were investigated using Spearman correlation and subsequent multiple regression with stepwise backward elimination to find potential predictors.

RESULTS

Patient Population

All 60 patients participating in the original study were also included in the present substudy. The baseline characteristics including cardiovascular risk factors are shown in Table 1. Framingham risk score describing the 10-y risk for cardiovascular disease, as calculated from BMI, showed 22% of patients with less than 10% risk (n = 13), 17% with 10%–20% risk (n = 10), 20% with 20%–30% risk (n = 12), and 27% with greater than 30% risk (n = 16). For 15% of the patients (n = 9), it was not possible to calculate the risk, because of missing data. Forty-five percent (n = 27) had a coronary calcium score of zero, whereas 15% (n = 9) had a score above 400.

PET/CT with ^{64}Cu-DOTATATE and ^{68}Ga-DOTATOC

On the Bland–Altman plot, the comparison of the uptake of the 2 tracers (Fig. 2A) showed that ^{64}Cu-DOTATATE had a significantly higher uptake value than ^{68}Ga-DOTATOC when calculated as whole-artery SUV_{max} ($P < 0.001$). The 95% limits of agreement were from −2.3 to 5.7. The uptake of ^{64}Cu-DOTATATE was

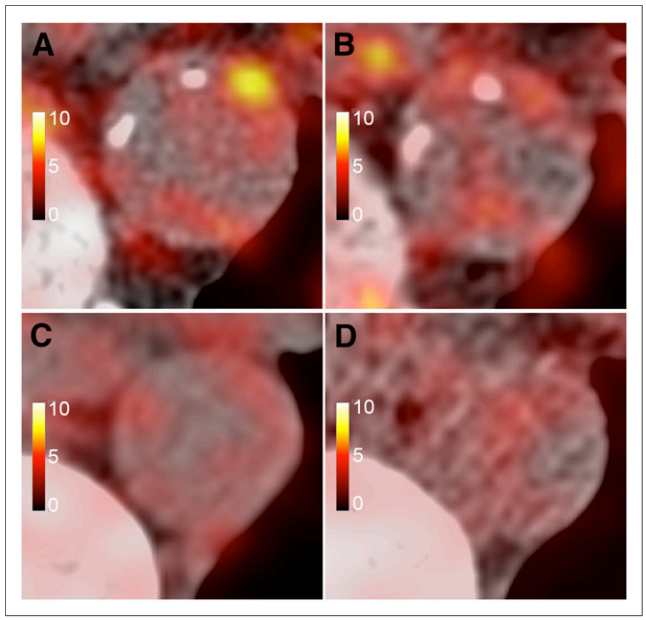

FIGURE 3. Examples of PET/CT fusion showing uptake of ^{64}Cu-DOTATATE (A and C) and ^{68}Ga-DOTATOC (B and D). Patient in A and B is 67-y-old man with Framingham risk score of 30. Images show high focal uptake in thoracic aorta on ^{64}Cu-DOTATATE PET (A), whereas same location on ^{68}Ga-DOTATOC PET is more blurred (B). Patient in C and D is 31-y-old woman with Framingham risk score of 2. Images show lower and more diffuse uptake with both tracers.

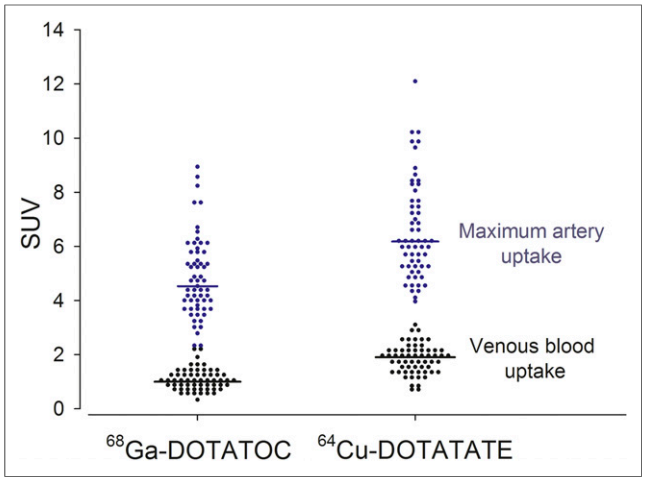

FIGURE 4. SUVs of ^{68}Ga-DOTATOC and ^{64}Cu-DOTATATE in arteries (blue) and superior cava vein (black). Data are paired, and each patient is represented with dot in each of the 4 categories. Median uptake is shown in bold lines.

also significantly higher measured as whole-artery SUV_{mean} ($P < 0.001$), with 95% limits of agreement from −0.5 to 1.1 (Fig. 2B). Representative images of high focal and low diffuse uptake of the 2 tracers are shown in Figure 3. Also, venous SUV was higher with ^{64}Cu-DOTATATE than with ^{68}Ga-DOTATOC, and the numeric difference between arterial and venous uptake was highest with ^{64}Cu-DOTATATE (Fig. 4).

The mean difference between uptake of the tracers (SUV) was also calculated in the 5 regions, respectively, with significant results in all 5 artery segments, showing higher uptake of ^{64}Cu-DOTATATE, as seen in Table 2.

Correlation with Risk Factors

The association between tracer uptake and risk factors was investigated using both SUV_{mean} and SUV_{max} in the 5 artery segments, for both tracers. We found an overall significant association between maximum ^{64}Cu-DOTATATE uptake (whole-artery SUV_{max}) and Framingham risk score ($r = 0.4$; $P = 0.004$, Fig. 5B), whereas maximum ^{68}Ga-DOTATOC (whole-artery SUV_{max}) did not correlate with Framingham risk score ($P = 0.3$, Fig. 5A). Whole-artery SUV_{mean} did not correlate with Framingham risk score, neither with ^{64}Cu-DOTATATE ($r = 0.1$; $P = 0.4$) nor with ^{68}Ga-DOTATOC ($r = -0.3$; $P = 0.1$). Similar results were found when TBR was used rather than SUV, but with a lower correlation between maximum ^{64}Cu-DOTATATE uptake (whole-artery maximum TBR) and Framingham risk score ($r = 0.3$; $P = 0.04$), and no correlation between Framingham risk score and ^{68}Ga-DOTATOC uptake.

The association between maximum ^{64}Cu-DOTATATE uptake and Framingham risk score was consistently found in 3 of the 5 vascular regions (descending thoracic aorta, proximal part of the abdominal aorta, and iliac arteries), whereas ^{68}Ga-DOTATOC was only inversely correlated with Framingham risk score in 1 region (distal part of the abdominal aorta) (Table 3).

Multiple regression including sex, age, BMI, diabetes, smoking, systolic blood pressure, coronary calcium score, and treatment for hypertension and treatment for hypercholesterolemia showed that BMI, smoking, diabetes, and coronary calcium score were independent predictors of SUV_{max} with ^{64}Cu-DOTATATE ($P < 0.001$, $P = 0.01$, $P = 0.005$, and $P = 0.03$, respectively).

DISCUSSION

We present here the first comparison of arterial uptake of ^{64}Cu-DOTATATE with ^{68}Ga-DOTATOC in a population unselected for cardiovascular risk profile using hybrid PET/CT. We found a higher uptake of ^{64}Cu-DOTATATE and wide limits of agreement for maximum uptake (SUV_{max}) of the 2 tracers. In addition, we found results in support of an association between ^{64}Cu-DOTATATE and cardiovascular risk factors suggesting this radiotracer as a potential noninvasive biomarker of cardiovascular risk. This result supports our recent finding in patients with severe carotid stenosis in whom ^{64}Cu-DOTATATE uptake in excised carotid plaques was associated with the gene expression of a marker of alternatively activated macrophages (*9*). Together, it therefore may seem that ^{64}Cu-DOTATATE may be valuable in imaging of atherosclerosis both in patients with and in patients without known atherosclerotic cardiovascular disease.

The use of the PET technique to visualize atherosclerosis was initiated by the finding that patients scanned after injection of FDG, labeled with the radionuclide ^{18}F, for tumor visualization also showed arterial uptake of the tracer (*16*). The first clinical study with PET imaging of atherosclerosis, published in 2002 (*17*), was consequently performed using ^{18}F-FDG, which is a marker for uptake of glucose and hereby metabolism in tissue. The uptake of ^{18}F-FDG was later shown to correlate significantly with plaque macrophage content, with other circulating inflammatory biomarkers (*18–21*) and known cardiovascular risk

TABLE 2
Mean Difference Between ^{64}Cu-DOTATATE and ^{68}Ga-DOTATOC Uptake in Each Region

Region	SUV_{mean}		SUV_{max}	
	Mean difference*	*P*	Mean difference*	*P*
Aortic arch	0.5	0.007	2.3	<0.001
Thoracic aorta	0.3	<0.001	2.2	<0.001
Proximal abdominal aorta	0.3	<0.001	1.1	0.04
Distal abdominal aorta	0.2	<0.001	1.6	0.003
Iliac arteries	0.2	<0.001	1.4	<0.001

*^{64}Cu-DOTATATE uptake minus ^{68}Ga-DOTATOC uptake.

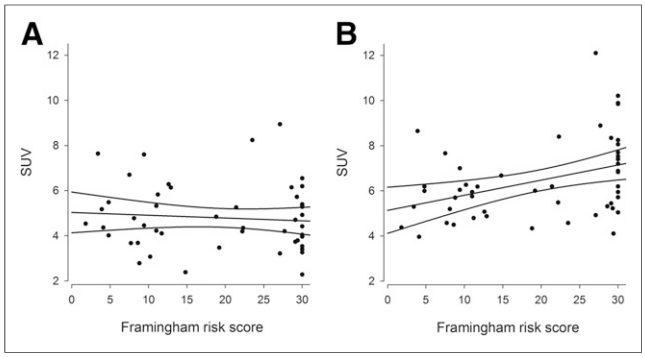

FIGURE 5. Correlation between Framingham risk score and ^{68}Ga-DOTATOC uptake (A) and whole-artery ^{64}Cu-DOTATATE uptake (B).

factors (*6,22*). Therefore, hope has risen that ^{18}F-FDG might be used to evaluate therapeutic intervention (*23*). After the optimistic results that PET scans with ^{18}F-FDG have given, additional and more specific tracers have been developed, for example, tracers targeting macrophages. Although ^{18}F-FDG visualizes the metabolism of the cell and therefore the physiologic state of inflammation that a given cell in an atherosclerotic plaque is in, targeting a macrophage-expressed receptor could be a more specific tracer.

The aim of this study was to compare the uptake of 2 somatostatin receptor–binding PET tracers in large arteries and evaluate their use in PET/CT in the assessment of atherosclerosis. These tracers have earlier been used and compared in connection with cancer diagnostics, primarily neuroendocrine tumors (*24–26*). Furthermore, ^{68}Ga-DOTATATE has previously been assessed in relation to inflammation in the aorta and compared with ^{18}F-FDG (*27*). There are to our knowledge no studies that have compared the uptake of DOTATOC and DOTATATE in the aorta in addition to their possible role for risk evaluation.

Both DOTATOC and DOTATATE are somatostatin analogs conjugated with the chelator abbreviated DOTA, which hereafter are labeled with radiopharmaceuticals to be visualized on PET scans. The difference between the peptides is a replacement of octreotide C-terminal threoninol (DOTATOC) to the natural amino acid threonine, which produces octreotate (DOTATATE). When the peptides are labeled with ^{67}Ga, they both bind to the somatostatin receptor 2 with exceptional affinity; however, binding is highest for DOTATATE (*7*). On the basis of this and previous studies (*7,14,28,29*), we would expect an uptake of both tracers in regions with plaque formations and furthermore that, in our case, the ^{64}Cu-labeled DOTATATE would show higher focal uptake in the aorta than ^{68}Ga-DOTATOC.

We found a consistent difference between uptake of the tracers calculated as SUV_{max}, SUV_{mean}, maximum TBR, and mean TBR in all tested vascular regions. All SUV results show highest uptake of ^{64}Cu-DOTATATE. This was not unexpected, because ^{64}Cu has a shorter positron range (~1 mm) than ^{68}Ga (~4 mm). ^{64}Cu is thus less sensitive to both spillover and partial-volume loss. In concordance with this, we found especially SUV_{max} to have wide limits of agreement when ^{64}Cu-DOTATATE was compared with ^{68}Ga-DOTATOC. The difference in affinity between the tracers is also consistent with the higher SUV of DOTATATE than DOTATOC in the vascular regions. It should be acknowledged that a higher PET signal is preferable when assessing plaques, because of their small dimensions.

We also investigated association between the uptake of tracer and classic cardiovascular risk factors. A positive correlation reinforces the theory that individuals with a certain behavior and phenotype, known to have higher risk of developing atherosclerosis, also would have high tracer uptake (*30*).

The results showed an association between Framingham risk score and overall maximum ^{64}Cu-DOTATATE uptake whereas overall ^{68}Ga-DOTATOC uptake was not associated with the risk score. This is important methodologic information because studies of atherosclerosis using ^{68}Ga-labeled somatostatin receptor tracers may overlook true differences. Previous studies have shown a high congruence between ^{68}Ga-DOTATATE and ^{68}Ga-DOTATOC binding (*24,31*). Therefore, it is our hypothesis that the difference in both measured vessel wall uptake (Fig. 2) and Framingham risk correlation (Fig. 5) is primarily caused by the difference in radiotracer emission energy between ^{64}Cu and ^{68}Ga and thus related to the spatial resolution of the examination rather than a physiologic difference in tracer binding. Still, other studies have shown a correlation between DOTATATE labeled with ^{68}Ga and risk factors (*6,8,27*). However, more atherosclerotic vessels in these studies may be the cause hereof.

As expected, we found only an association between Framingham risk score and SUV_{max}, whereas SUV_{mean} did not correlate. This is in concordance with previous studies (*6,8,27*) and further supports the hypothesis that vascular ^{64}Cu-DOTATATE uptake is heterogeneous and could serve as a marker of more advanced and potentially more vulnerable lesions. Similarly, we have previously found heterogeneous uptake of ^{18}F-FDG in atherosclerotic carotid plaques (*18*).

A limitation of the study is the lack of histologic samples to validate that the uptake of tracer is actually from vascular lesions

TABLE 3
Correlations Between Framingham Risk Score and Maximum Tracer Uptake in 5 Regions

Region	^{64}Cu-DOTATATE		^{68}Ga-DOTATOC	
	Spearman rho	*P*	Spearman rho	*P*
Aortic arch	0.30	0.36	0.03	0.8
Thoracic aorta	0.36	0.01	0.18	0.2
Proximal abdominal aorta	0.43	0.002	−0.07	0.6
Distal abdominal aorta	0.23	0.1	−0.35	0.013
Iliac arteries	0.37	0.008	−0.04	0.8

and to what cell type the tracer is binding. Therefore, prospective studies are warranted with other (nononcologic) and larger patient groups to further validate the clinical use of PET/CT with somatostatin receptor–binding tracers in the assessment of atherosclerosis (*8*).

CONCLUSION

In this study of 2 somatostatin receptor–binding tracers for PET/CT, we found a higher vascular uptake of the ^{64}Cu-labeled DOTATATE than ^{68}Ga-DOTATOC. Furthermore, results showed a significant correlation of Framingham risk score with uptake of ^{64}Cu-DOTATATE, which was driven by smoking, BMI, and diabetes. No such correlation was found with ^{68}Ga-DOTATOC. We suggest that ^{64}Cu-DOTATATE seems suitable for the assessment of atherosclerosis even in the subclinical stages, but prospective studies to further validate this are required.

DISCLOSURE

The costs of publication of this article were defrayed in part by the payment of page charges. Therefore, and solely to indicate this fact, this article is hereby marked "advertisement" in accordance with 18 USC section 1734. This work was supported by unrestricted grants from the John & Birthe Meyer Foundation, the National Advanced Technology Foundation, Danish Medical Research Council, Rigshospitalets Research Foundation, Svend Andersen Foundation, AP Møller Foundation, Novo Nordisk Foundation, and Lundbeck Foundation. No other potential conflict of interest relevant to this article was reported.

ACKNOWLEDGMENTS

We thank the staff in the PET center for their skillful assistance.

REFERENCES

1. Ross R. Atherosclerosis: an inflammatory disease. *N Engl J Med.* 1999;340:115–126.
2. Davies JR, Rudd JH, Weissberg PL. Molecular and metabolic imaging of atherosclerosis. *J Nucl Med.* 2004;45:1898–1907.
3. Gallino A, Stuber M, Crea F, et al. "In vivo" imaging of atherosclerosis. *Atherosclerosis.* 2012;224:25–36.
4. Li X, Bauer W, Kreissl MC, et al. Specific somatostatin receptor II expression in arterial plaque: ^{68}Ga-DOTATATE autoradiographic, immunohistochemical and flow cytometric studies in apoE-deficient mice. *Atherosclerosis.* 2013;230:33–39.
5. Armani C, Catalani E, Balbarini A, Bagnoli P, Cervia D. Expression, pharmacology, and functional role of somatostatin receptor subtypes 1 and 2 in human macrophages. *J Leukoc Biol.* 2007;81:845–855.
6. Rominger A, Saam T, Vogl E, et al. In vivo imaging of macrophage activity in the coronary arteries using ^{68}Ga-DOTATATE PET/CT: correlation with coronary calcium burden and risk factors. *J Nucl Med.* 2010;51:193–197.
7. Reubi JC, Schar JC, Waser B, et al. Affinity profiles for human somatostatin receptor subtypes SST1-SST5 of somatostatin radiotracers selected for scintigraphic and radiotherapeutic use. *Eur J Nucl Med.* 2000;27:273–282.
8. Schatka I, Wollenweber T, Haense C, Brunz F, Gratz KF, Bengel FM. Peptide receptor-targeted radionuclide therapy alters inflammation in atherosclerotic plaques. *J Am Coll Cardiol.* 2013;62:2344–2345.
9. Pedersen SF, Sandholt B, Keller S, et al. ^{64}Cu-DOTATATE PET/MR for detection of activated macrophages in carotid atherosclerotic plaques: studies in patients undergoing endarterectomy. *Arterioscler Thromb Vasc Biol.* 2015;35:1696–1703.
10. Velikyan I. Prospective of ^{68}Ga-radiopharmaceutical development. *Theranostics.* 2013;4:47–80.
11. Rice SL, Roney CA, Daumar P, Lewis JS. The next generation of positron emission tomography radiopharmaceuticals in oncology. *Semin Nucl Med.* 2011;41:265–282.
12. Li Z, Conti PS. Radiopharmaceutical chemistry for positron emission tomography. *Adv Drug Deliv Rev.* 2010;62:1031–1051.
13. Fani M, Andre JP, Maecke HR. ^{68}Ga-PET: a powerful generator-based alternative to cyclotron-based PET radiopharmaceuticals. *Contrast Media Mol Imaging.* 2008;3:67–77.
14. Wadas TJ, Wong EH, Weisman GR, Anderson CJ. Coordinating radiometals of copper, gallium, indium, yttrium, and zirconium for PET and SPECT imaging of disease. *Chem Rev.* 2010;110:2858–2902.
15. D'Agostino RB Sr, Vasan RS, Pencina MJ, et al. General cardiovascular risk profile for use in primary care: the Framingham Heart Study. *Circulation.* 2008;117:743–753.
16. Yun M, Yeh D, Araujo LI, Jang S, Newberg A, Alavi A. F-18 FDG uptake in the large arteries: a new observation. *Clin Nucl Med.* 2001;26:314–319.
17. Rudd JH, Warburton EA, Fryer TD, et al. Imaging atherosclerotic plaque inflammation with [^{18}F]-fluorodeoxyglucose positron emission tomography. *Circulation.* 2002;105:2708–2711.
18. Pedersen SF, Graebe M, Fisker Hag AM, Hojgaard L, Sillesen H, Kjaer A. Gene expression and 18FDG uptake in atherosclerotic carotid plaques. *Nucl Med Commun.* 2010;31:423–429.
19. Graebe M, Pedersen SF, Borgwardt L, Hojgaard L, Sillesen H, Kjaer A. Molecular pathology in vulnerable carotid plaques: correlation with [18]-fluorodeoxyglucose positron emission tomography (FDG-PET). *Eur J Vasc Endovasc Surg.* 2009;37:714–721.
20. Hag AM, Pedersen SF, Christoffersen C, et al. ^{18}F-FDG PET imaging of murine atherosclerosis: association with gene expression of key molecular markers. *PLoS One.* 2012;7:e50908.
21. Pedersen SF, Graebe M, Hag AM, Hojgaard L, Sillesen H, Kjaer A. ^{18}F-FDG imaging of human atherosclerotic carotid plaques reflects gene expression of the key hypoxia marker HIF-1alpha. *Am J Nucl Med Mol Imaging.* 2013;3:384–392.
22. Yun M, Jang S, Cucchiara A, Newberg AB, Alavi A. ^{18}F FDG uptake in the large arteries: a correlation study with the atherogenic risk factors. *Semin Nucl Med.* 2002;32:70–76.
23. Camici PG, Rimoldi OE, Gaemperli O, Libby P. Non-invasive anatomic and functional imaging of vascular inflammation and unstable plaque. *Eur Heart J.* 2012;33:1309–1317.
24. Pfeifer A, Knigge U, Mortensen J, et al. Clinical PET of neuroendocrine tumors using ^{64}Cu-DOTATATE: first-in-humans study. *J Nucl Med.* 2012;53:1207–1215.
25. Velikyan I, Sundin A, Sorensen J, et al. Quantitative and qualitative intrapatient comparison of ^{68}Ga-DOTATOC and ^{68}Ga-DOTATATE: net uptake rate for accurate quantification. *J Nucl Med.* 2014;55:204–210.
26. Johnbeck CB, Knigge U, Kjaer A. PET tracers for somatostatin receptor imaging of neuroendocrine tumors: current status and review of the literature. *Future Oncol.* 2014;10:2259–2277.
27. Li X, Samnick S, Lapa C, et al. ^{68}Ga-DOTATATE PET/CT for the detection of inflammation of large arteries: correlation with^{18}F-FDG, calcium burden and risk factors. *EJNMMI Res.* 2012;2:52.
28. Yang J, Kan Y, Ge BH, Yuan L, Li C, Zhao W. Diagnostic role of gallium-68 DOTATOC and gallium-68 DOTATATE PET in patients with neuroendocrine tumors: a meta-analysis. *Acta Radiol.* 2014;55:389–398.
29. Randolph GJ. Mechanisms that regulate macrophage burden in atherosclerosis. *Circ Res.* 2014;114:1757–1771.
30. Pearson TA, Mensah GA, Alexander RW, et al. Markers of inflammation and cardiovascular disease: application to clinical and public health practice: a statement for healthcare professionals from the Centers for Disease Control and Prevention and the American Heart Association. *Circulation.* 2003;107:499–511.
31. Virgolini I, Ambrosini V, Bomanji JB, et al. Procedure guidelines for PET/CT tumour imaging with ^{68}Ga-DOTA-conjugated peptides: ^{68}Ga-DOTA-TOC, ^{68}Ga-DOTA-NOC, ^{68}Ga-DOTA-TATE. *Eur J Nucl Med Mol Imaging.* 2010;37:2004–2010.